Inorg. Chem. **2008**, *47*, 4682−4690

Theoretical and Experimental Studies of Diruthenium Tetracarboxylates Structure, Spectroscopy, and Electrochemistry

Maria Ana Castro,[†] Adrian E. Roitberg,*[,‡] and Fabio D. Cukiernik*[,†,§]

INQUIMAE, Departamento de Química Inorgánica, Analítica y Química Física, Facultad de Ciencias Exactas y Naturales, Universidad de Buenos Aires, Pab. II, Ciudad Universitaria, C1428EHA Buenos Aires, Argentina, Quantum Theory Project, University of Florida, 32611 Gainesville, Florida 32611, and Instituto de Ciencias, Universidad Nacional de General Sarmiento, J. M. Gutierrez 1150, B1613GSX, Los Polvorines, Prov. Buenos Aires, Argentina

Received December 28, 2007

Quantum mechanical calculations at the density functional theory (DFT) level have been performed on diruthenium tetracarboxylates of different levels of molecular complexity: from unsolvated monomers to oligomers. The agreement between the calculated and experimental molecular structures and vibrational modes of the simple $[Ru_2(\mu\text{-}O_2CCH_3)_4]^{0/+}$ and $[Ru_2(\mu\text{-}O_2CCH_3)_4(H_2O)_2]^{0/+}$ systems made us confident in our calculation methodology. Therefore, it has been applied to the analysis of two different kinds of properties of these compounds: the trends in the UV/vis spectroscopy and electrochemistry along the $[Ru_2(\mu\text{-}O_2CCH_3)_4X_2]^-$ ($X = Cl^-$, Br^-, I^-) series, and the crystalline polymorphism related to the polymeric strand conformation in extended $Ru_2(\mu\text{-}O_2CR)_4Cl$ compounds. For the $[Ru_2(\mu\text{-}O_2CCH_3)_4X_2]^-$ series, we report new spectroscopic and electrochemical results and interpret the trends on the basis of time dependent DFT-polarized continuum model calculations, local charge and spin analysis, and X donor properties. As far as the polymeric conformation is concerned, it has been previously suggested that the Ru−Cl−Ru angle results from a compromise between packing, orbital overlap, and microsegregation. Our calculations on $[Ru_2(\mu\text{-}O_2CCH_3)_4Cl]_2Cl^-$ and $[Ru_2(\mu\text{-}O_2CCH_3)_4Cl]_3Cl^-$ oligomers provide insights on the influence of the first two factors on the strand conformation and allows a suggestion on what is the equatorial aliphatic chain's influence on this issue.

Introduction

Bimetallic carboxylates with lantern-like molecular structure are a class of compounds widely spread among different fields of modern coordination chemistry: magnetic interactions between metal centers,[1] magnetic materials,[2,3] metal-containing liquid crystals,[4−6] enantioselective catalysis,[7] and biochemical applications.[8,9] Interest has recently been focused on the use of bimetallic carboxylates or related compounds[10] as building blocks for both supramolecular arrays[11−13] and advanced materials.[2,3,6a,14]

Among the wide variety of metals that form lantern-like bimetallic carboxylates, ruthenium derivatives are especially interesting for they exhibit two accessible redox states ($Ru_2^{(II,II)}$, $Ru_2^{(II,III)}$). Both redox states exhibit multiple bonds between ruthenium atoms (bond order 2 and 2.5, respectively), and both are paramagnetic because of the presence of 2 or 3 unpaired electrons. These very attractive molecular properties were experimentally studied (electronic spectros-

* To whom correspondence should be addressed. E-mail: fabioc@qi.fcen.uba.ar (F.D.C.), roitberg@ufl.edu (A.E.R.).
† Universidad de Buenos Aires.
‡ University of Florida.
§ Universidad Nacional de General Sarmiento.

(1) Bleaney, B.; Bowers, K. D. *Proc. R. Soc. London* **1952**, *A214*, 451.
(2) (a) Vos, T. E.; Liao, Y.; Shum, W. W.; Her, J. H.; Stephens, P. W.; Reiff, W. M.; Miller, J. S. *J. Am. Chem. Soc.* **2004**, *126*, 11630. (b) Vos, T. E.; Miller, J. S. *Angew. Chem., Int. Ed.* **2005**, *44*, 2416.
(3) Mikuriya, M.; Yoshioka, D.; Handa, M. *Coord. Chem. Rev.* **2006**, *250*, 2194.
(4) (a) Marchon, J. C.; Maldivi, P.; Giroud, A. M.; Guillon, D.; Ibn-Elhaj, M.; Skoulios, A., In *Nanostructures Based on Molecular Materials*; Göpel, W., Ziegler, Ch., Ed.; VCH:Weinheim, 1992; p 285. (b) Marchon, J. C.; Maldivi, P.; Giroud-Godquin, A. M.; Guillon, D.; Skoulios, A.; Strommen, D. P. *Philos. Trans. R. Soc. London* **1990**, *A330*, 109. (c) Barberá, J.; Esteruelas, M. A.; Levelut, A. M.; Oro, L. A.; Serrano, J. L.; Sola, E. *Inorg. Chem.* **1992**, *31*, 732. (d) Baxter, D. V.; Cayton, R. H.; Chisholm, M. H.; Huffman, J. C.; Putilina, E. F.; Tagg, S. L.; Wesemann, J. L.; Zwanziger, J. W.; Darrington, F. D. *J. Am. Chem. Soc.* **1994**, *116*, 4551. (e) Rusjan, M.; Donnio, B.; Guillon, D.; Cukiernik, F. D. *Chem. Mater.* **2002**, *14*, 1564.

10.1021/ic702505z CCC: $40.75
Published on Web 05/06/2008

copy, vibrational spectroscopy, electrochemistry, and magnetic measurements). Together with crystallography[15–16] and a few theoretical calculations, those studies aimed to gain a better understanding of the electronic structure of these compounds. A very comprehensive review has been published by Aquino.[7,17]

The SCF-Xα-SW[18] calculations performed by Norman and co-workers[19] were a key early step in the assignment of the electronic structure of the ruthenium derivatives. They described for the first time the accidental near-degeneracy of the π^* and δ^* molecular orbitals (MOs) as a consequence of the different interactions the d_{xy}, d_{xz}, and d_{yz} Ru orbitals have with the carboxylate-centered ligand orbitals. That work was based on a fixed molecular geometry (taken from the wide database of crystallographic studies), as were the subsequent theoretical calculations on these Ru compounds[20–22] and most of the theoretical studies carried out in the 1970s and 1980s which aimed to establish the electronic structure of bimetallic carboxylates.[23] Only in recent years new calculations on bimetallic carboxylates, including molecular structure optimization and normal-mode analysis, have been conducted at the density functional theory (DFT) level,[24,25] but they deal almost exclusively with diamagnetic (closed shell) systems. No such study has been published on open-shell systems up to 2005, probably because of the convergence difficulties usually associated with such calculations. There exist two recent reports on DFT calculations on diruthenium carboxylates including geometry optimization: a paper by Chisholm and co-workers,[26] who aimed to examine the electronic structure of equatorially linked (oxalate bridged) extended bimetallic carboxylates, and a paper by Sizova and co-workers,[27] who studied (II,II) carboxylates axially coordinated by NO.

On the basis of the peculiar electronic structure of the molecular unit, we have been interested for several years in the synthesis of new materials based on diruthenium tetracarboxylates. We have succeeded to establish molecular structure–property relationships regarding their mesomorphic character,[5a,28,29] magnetic behavior,[30,31] and thermal stability[32] and developed models for explaining some structural features of their mesophases[5a,33] or the magnetic interactions.[21,31] We are now interested in the design of new materials, based on diruthenium carboxylates, that exhibit a high degree of communication between adjacent (axially linked) bimetallic centers. Instead of synthesizing, characterizing, orienting, and measuring a large number of such compounds to systematically search for the best bimetallic center/equatorial ligands/axial ligands combination for the desired property, we have decided to undertake a computational exploration on this issue. As the aimed at collective properties could be concomitant with particular structural features, we cannot simply extrapolate the structural parameters of the already known systems, so we will perform ab initio calculations including geometry optimization.

One of the aims of this paper is to validate the quantum mechanics (QM) methodology chosen for the analysis: level of theory (DFT),[34–36] appropriate functionals,[37,38] and basis sets. We selected three relevant kinds of properties to predict

(5) (a) Cukiernik, F. D.; Ibn-Elhaj, M.; Chaia, Z. D.; Marchon, J. C.; Giroud-Godquin, A. M.; Guillon, D.; Skoulios, A.; Maldivi, P. *Chem. Mater.* **1998**, *10*, 83. (b) Bonnet, L.; Cukiernik, F. D.; Maldivi, P.; Giroud-Godquin, A. M.; Marchon, J. C.; Ibn-Elhaj, M.; Guillon, D.; Skoulios, A. *Chem. Mater.* **1994**, *6*, 31. (c) Caplan, J. F.; Murphy, C. C.; Swansburg, S.; Lemieux, R. P.; Cameron, S.; Aquino, M. A. S. *Can. J. Chem.* **1998**, *76*, 1520.

(6) (a) Aquino, M. A. S. *Coord. Chem. Rev.* **1998**, *170*, 141.

(7) (a) Ikota, N.; Takamura, N.; Young, S. D.; Ganem, B. *Tetrahedron Lett.* **1981**, *22*, 4163. (b) Callot, H. J.; Metz, F. *Tetrahedron* **1985**, *41*, 4495.

(8) (a) Kozlevcar, B.; Fajfar, S.; Petric, M.; Pohleven, F.; Segedin, P. *Acta Chim. Slov.* **1996**, *43*, 385. (b) Bear, J. L.; Howard, R. A.; Dennis, A. M. *Curr. Chemother.* **1978**, 1321.

(9) (a) Andrade, A.; Namora, S. F.; Woisky, R. G.; Wiezel, G.; Najjar, R.; Sertié, J. A. A.; de Oliveira Silva, D. *J. Inorg. Biochem.* **2000**, *81*, 23. (b) van Rensburg, C. E. J.; Kreft, E.; Swarts, J. C.; Darymple, S. R.; MacDonald, D. M.; Cooke, M. W.; Aquino, M. A. S. *Anticancer Res.* **2002**, *22*, 889.

(10) Cotton, F. A.; Murillo, C. A.; Walton, R. A. *Multiple Bonds Between Metal Atoms*, 3rd ed.; Springer Science and Business Media: New York, 2005.

(11) Cotton, F. A.; Lin, C.; Murillo, C. A. *Proc. Natl. Acad. Sci. U.S.A.* **2002**, *99*, 4810.

(12) Bonnar-Law, R. P.; Mc Grath, T. D.; Bickley, J. F.; Femoin, C.; Steiner, A. *Inorg. Chem. Commun.* **2001**, *4*, 16.

(13) Anagaridis, P.; Berry, J. F.; Cotton, F. A.; Murillo, C. A.; Wang, X. *J. Am. Chem. Soc.* **2003**, *125*, 10327.

(14) Barral, M. C.; Gallo, T.; Herrero, S.; Jimenez-Aparicio, R.; Torres, M. R.; Urbanos, F. A. *Inorg. Chem.* **2006**, *45*, 3639.

(15) Donnio, B.; Guillon, D.; Deschenaux, R.; Bruce D. W. In *Comprehensive Coordination Chemistry*; Mc Cleverty, J., Meyer, T. J., Eds.; Elsevier Pergamon: Amsterdam, 2004; Vol. 7, p 359.

(16) Pruchnik, F. P.; Jakimowicz, P.; Civnik, Z.; Stanislawek, K.; Oro, L. A.; Tejel, C.; Ciriano, M. A. *Inorg. Chem. Commun.* **2001**, *4*, 19.

(17) Aquino, M. A. S. *Coord. Chem. Rev.* **2004**, *248*, 1025.

(18) (a) Slater, J. C. *Quantum Theory of Molecules and Solids*; McGraw-Hill: New York, N.Y., 1974; Vol. *4*. (b) Johnson, K. H. *Annu. Rev. Phys. Chem.* **1975**, *26*, 39.

(19) Norman, J. G.; Renzoni, G. E.; Case, D. A. *J. Am. Chem. Soc.* **1979**, *101*, 5256.

(20) Quelch, G. E.; Hillier, I. H.; Guest, M. F. *J. Chem. Soc., Dalton Trans.* **1990**, 3075.

(21) Estiú, G.; Cukiernik, F. D.; Maldivi, P.; Poizat, O. *Inorg. Chem.* **1999**, *38*, 3030.

(22) Wesemann, J. L.; Chisholm, M. H. *Inorg. Chem.* **1997**, *36*, 3258.

(23) (a) Norman, J. G.; Kolari, H. J.; Gray, H. B.; Trogler, W. C. *Inorg. Chem.* **1977**, *16*, 987. (b) Benard, M. *J. Am. Chem. Soc.* **1978**, *10*, 2354.

(24) Cotton, F. A.; Cowley, A. H.; Feng, X. *J. Am. Chem. Soc.* **1998**, *120*, 1795.

(25) (a) Cotton, F. A.; Feng, X. *J. Am. Chem. Soc.* **1997**, *119*, 7514. (b) Cotton, F. A.; Feng, X. *J. Am. Chem. Soc.* **1998**, *120*, 3387.

(26) Bursten, B. E.; Chisholm, M. H.; Acchioli, J. S. *Inorg. Chem.* **2005**, *44*, 5571.

(27) Sizova, O. V.; Skripnikov, L. V.; Sokolov, A. Y.; Lyubimova, O. O. *J. Struct. Chem.* **2007**, *48*, 28.

(28) Chaia, Z.; Zelcer, A.; Donnio, B.; Rusjan, M; Cukiernik, F. D.; Guillon, D. *Liq. Cryst.* **2004**, *31*, 1019.

(29) Rusjan, M.; Donnio, B.; Heinrich, B.; Cukiernik, F. D.; Guillon, D. *Langmuir* **2002**, *18*, 10116.

(30) Cukiernik, F. D.; Giroud-Godquin, A. M.; Maldivi, P.; Marchon, J. C. *Inorg. Chim. Acta* **1994**, *215*, 203.

(31) Cukiernik, F. D.; Luneau, D.; Marchon, J. C.; Maldivi, P. *Inorg. Chem.* **1998**, *37*, 3698.

(32) (a) Rusjan, M. C.; Sileo, E. E.; Cukiernik, F. D. *Solid State Ionics* **1999**, *124*, 143. (b) Rusjan, M. C.; Sileo, E. E.; Cukiernik, F. D. *Solid State Ionics* **2003**, *159*, 389.

(33) Chaia, Z.; Heinrich, B.; Cukiernik, F.; Guillon, D. *Mol. Cryst. Liq. Cryst.* **1999**, *330*, 213.

(34) (a) Ziegler, T. *Chem. Rev.* **1991**, *91*, 651. (b) *Theory and applications of Density Functional approaches to Chemistry*; Labanowski, J., Andzelm, J., Eds.; Springer-Verlag: Berlin, 1990.

(35) (a) Li, J.; Schreckenbach, G.; Ziegler, T. *J. Am. Chem. Soc.* **1995**, *117*, 486. (b) Daul, C.; Baerenas, E. J.; Vernooijs, P. *Inorg. Chem.* **1994**, *33*, 3538.

(36) Cotton, F. A.; Feng, X. *J. Am. Chem. Soc.* **1997**, *119*, 7514.

(37) (a) Perdew, P. W. *Phys. Rev.* **1986**, *B33*, 8800. (*Phys. Rev.*, **1986**, *B34*, 7406 (erratum)). (b) Perdew, P. W. *Phys. Rev.* **1986**, *B33*, 8822.

and to measure their agreement with the experimental results. A second important aim is to use these calculations as insights to understand some features regarding physicochemical properties of these compounds whose variations have been experimentally established but not yet firmly analyzed or fully explained. We will focus on two different problems: (i) trends in spectroscopy and electrochemistry of binuclear bis-adducts and (ii) crystalline polymorphism and the supramolecular structure of polymeric derivatives. We also report new experimental data that was needed to have complete sets of data for trend analysis.

Our results are then organized in this paper in three sections. In the first one, we compute molecular geometries, electronic structure, and vibrational normal modes of the already studied $[Ru_2(\mu\text{-}O_2CCH_3)_4]^+$, $[Ru_2(\mu\text{-}O_2CCH_3)_4(H_2O)_2]^+$, $[Ru_2(\mu\text{-}O_2CCH_3)_4]$, and $[Ru_2(\mu\text{-}O_2CCH_3)_4(H_2O)_2]$ moieties, considered here as key building blocks for extended systems. In the second section, we analyze systematic variations of selected properties along the $[Ru_2(\mu\text{-}O_2CCH_3)_4X_2]^-$ series (X = chloride, bromide, and iodide), namely, the molecular structure, vibrational normal modes, UV-vis spectra, and electrochemical potential trends. No such comparative study has been conducted up to this time on this series, with the only exception of a recent paper by Jimenez-Aparicio et al.,[39] which includes crystallographic studies on the bromide and iodide derivatives, describes the experimental trends in structural and spectroscopic features, but does not intend to interpret them. We add in this paper experimental information about the electrochemistry of this series and use the QM calculations as insights to rationalize the experimental trends. Finally, in the third section, we undertake the analysis of the conformation of $\cdots Ru_2-Cl-Ru_2\cdots$ strands in extended systems, an issue relevant to both the basic structural aspects of these compounds, their mesogenic properties, and their magnetic behavior. In the crystalline state, the experimental Ru−Cl−Ru angle has been found to vary from 115° to 180°; the influence of the nature of the equatorial aliphatic chain on this parameter not being clear, as different polymorphs have been found for some compounds. This angle has been shown to be the key parameter determining the extent of antiferromagnetic interaction in $Ru_2(\mu\text{-}O_2CR)_4Cl$ compounds.[3,31] The structural aspects of the liquid crystalline (LC) phase of long chain derivatives have been studied by a combination of different techniques such as X-ray diffraction (XRD) in the LC phase, local probes (resonant Raman, IR, molecular magnetism, EXAFS), volumetric studies, and crystalline structures of nonmesogenic analogues. On this basis, a model for the supramolecular organization of these phases has been proposed;[29,33,40] one of its central points is the zigzag nature of the polymeric $\cdots Ru_2-Cl-Ru_2\cdots$ strands, with an estimated angle consistent with a posteriori information obtained from crystallized homologues,[41] which can be modified by the addition of solvents.[29] Detailed explanations have been proposed neither for the crystalline polymorphism of $Ru_2(\mu\text{-}O_2CR)_4Cl$ compounds nor for the variations found in the Ru−Cl−Ru angle value with the nature of R or the aggregation state. It has been suggested,[29,40] that the Ru−Cl−Ru angle results from a compromise between packing, orbital overlap, and microsegregation; our calculations provide insights on the influence of the first two factors on the strand conformation.

Computational Methods

Theoretical ab initio calculations were performed with DFT as implemented in the Gaussian 03 program.[42] We used Becke's three parameter hybrid functional with the correlation functional of Lee, Yang and Parr formalized as the B3LYP hybrid functional.[43] Unrestricted open-shell calculations were performed in every case. Electrons of alpha and beta spins are independently described which results in a set of orbital energies and molecular orbitals for electrons of alpha spin (alpha manifold) and another one for electrons of beta spin (beta manifold).[44]

An effective core potential basis set LanL2DZ[45] was used as it presented the better compromise between accuracy and computational cost. All structures were fully optimized and harmonic frequency calculations were performed to establish the nature of the critical points (minimum or transition state). No symmetry constraints were used for the optimization.

The energies and intensities of the lowest 200 singlet–singlet electronic transitions were calculated with the time dependent DFT (TDDFT)[46] which covered the region up to 250 nm. The UV–vis spectra were plotted using the SWizard[47] program, using a Gaussian broadening model. The half-bandwidths were taken to be equal to 3000 cm^{-1}.

(38) (a) Becke, A. D. *Phys. Rev.* **1986**, *A38*, 3098. (b) Becke, A. D. *J. Chem. Phys.* **1993**, *98*, 5648.

(39) Barral, M. C.; Gonzalez-Prieto, R.; Herrero, S.; Jimenez-Aparicio, R.; Priego, J. L.; Torres, M. R.; Urbanos, F. A. *Polyhedron* **2005**, *24*, 239.

(40) (a) Chaia, Z. D. PhD Thesis, University of Buenos Aires, Buenos Aires, Argentina, 2002. (b) Rusjan, M. C. PhD Thesis, University of Buenos Aires, Buenos Aires, Argentina, 2003.

(41) Castro, M. A.; Rusjan, M.; Baggio, R.; Vega, D.; Piro, O.; Zelcer, A.; Chaia, Z.; Gomez, R.; Fagnola, A.; Persello, M. A.; Heinrich, B.; Donnio, B; Guillon, D.; Cukiernik, F. D. *Proceedings of the 9th Int. Symp. Metallomesogens*, Lake Arrowhead, CA, U.S.A., 2005.

(42) Frisch, M. J.; Trucks, G. W.; Schlegel, H. B.; Scuseria, G. E.; Robb, M. A.; Cheeseman, J. R.; Montgomery, Jr., J. A.; Vreven, T.; Kudin, K. N.; Burant, J. C.; Millam, J. M.; Iyengar, S. S.; Tomasi, J.; Barone, V.; Mennucci, B.; Cossi, M.; Scalmani, G.; Rega, N.; Petersson, G. A.; Nakatsuji, H.; Hada, M.; Ehara, M.; Toyota, K.; Fukuda, R.; Hasegawa, J.; Ishida, M.; Nakajima, T.; Honda, Y.; Kitao, O.; Nakai, H.; Klene, M.; Li, X.; Knox, J. E.; Hratchian, H. P.; Cross, J. B.; Bakken, V.; Adamo, C.; Jaramillo, J.; Gomperts, R.; Stratmann, R. E.; Yazyev, O.; Austin, A. J.; Cammi, R.; Pomelli, C.; Ochterski, J. W.; Ayala, P. Y.; Morokuma, K.; Voth, G. A.; Salvador, P.; Dannenberg, J. J.; Zakrzewski, V. G.; Dapprich, S.; Daniels, A. D.; Strain, M. C.; Farkas, O.; Malick, D. K.; Rabuck, A. D.; Raghavachari, K.; Foresman, J. B.; Ortiz, J. V.; Cui, Q.; Baboul, A. G.; Clifford, S.; Cioslowski, J.; Stefanov, B. B.; Liu, G.; Liashenko, A.; Piskorz, P.; Komaromi, I.; Martin, R. L.; Fox, D. J.; Keith, T.; Al-Laham, M. A.; Peng, C. Y.; Nanayakkara, A.; Challacombe, M.; Gill, P. M. W.; Johnson, B.; Chen, W.; Wong, M. W.; Gonzalez, C.; and Pople, J. A. *Gaussian 03*, Revision C.02; Gaussian, Inc.: Wallingford, CT, 2004.

(43) Becke, A. D. *J. Chem. Phys.* **1993**, *98*, 5648.

(44) Szabo, A.; Ostlund, N. S. *Modern Quantum Chemistry. Introduction to Advanced Electronic Structure Theory*, 3rd ed.; Dover Publications, Inc.: Mineola, NY, 1996.

(45) (a) Dunning, T. H., Jr.; Hay, P. J. In *Modern Theoretical Chemistry*; Schaefer, H. F., III; Plenum Press: New York, 1977; Vol. 3. (b) Hay, P. J.; Wadt, W. R. *J. Chem. Phys.* **1985**, *82*, 270. (c) Wadt, W. R.; Hay, P. J. *J. Chem. Phys.* **1985**, *82*, 284. (d) Hay, P. J.; Wadt, W. R. *J. Chem. Phys.* **1985**, *82*, 299.

(46) (a) Stratmann, R. E.; Scuseria, G. E.; Frisch, M. J. *J. Chem. Phys.* **1998**, *109*, 8218. (b) Bauernschmitt, R.; Ahlrichs, R. *Chem. Phys. Lett.* **1996**, *256*, 454. (c) Casida, M. E.; Jamorski, C.; Casida, K. C.; Salahub, D. R. *J. Chem. Phys.* **1998**, *108*, 4439.

(47) Gorelsky, S. I. *SWizard program*, revision 4.2; York University: Toronto, Canada, 1998; http://www.sg-chem.net/ (accessed June 2007).

Solvent effects were taken into account by means of the polarized continuum model (PCM) calculations using standard options of the PCM and cavity keywords. Acetonitrile ($\varepsilon = 36.64$) was used as solvent. Geometries were fully reoptimized. TDDFT-PCM[48] (polarized continuum model) calculations were performed considering the nonequilibrium version of the PCM algorithm.

Molecular structures and orbitals were visualized with the program MOLEKEL.[49]

Experimental Section

The species $[Ru_2(\mu\text{-}O_2CCH_3)_4X_2]^-$ (X = Cl^-, Br^-, I^-) have been formed in acetonitrile solution (approximately 2×10^{-4} M) by addition of an excess of tetrabutylammonium halide (TBAX) to the corresponding diruthenium acetates, $Ru_2(\mu\text{-}O_2CCH_3)_4X$, which were synthesized following literature methods.[39,50] UV–vis spectra were recorded on a HP 8452A diode array spectrophotometer in a 1-cm-path-length quartz cell. Electrochemical data were obtained by cyclic voltammetry (CV) where a glassy carbon disk working electrode, a platinum coil auxiliary electrode, and a silver wire quasi-reference electrode were mounted in a single-compartment-cell configuration. The potential of the working electrode was controlled with a commercial potentiostat TEQ-03. A cyclic voltammogram was obtained by dissolving approximately 1 mM of the complex in acetonitrile containing 0.1 M of the corresponding TBAX as the supporting electrolyte. Decamethylferrocene (DMFc) was added as an internal reference. IUPAC recommends the ferrocene/ferrocinium (Fc/Fc^+) couple as a reference[51] but the presence of iodide ($E = -0.21$ V vs Fc) in one of the supporting electrolytes prevented its utilization.

Synthesis of $Ru_2(\mu\text{-}O_2CCH_3)_4Cl$. A 5.6 mmole quantity of $RuCl_3.3H_2O$ (Aldrich) and 45 mmole of anhydrous lithium chloride were added to a mixture of glacial acetic acid (65 mL) and acetic anhydride (14 mL). The solution was refluxed for 24–26 h in a slow stream of oxygen. After cooling to room temperature, the red brown salt was collected, washed with ether, and dried in vacuo.

Synthesis of $Ru_2(\mu\text{-}O_2CCH_3)_4X$ (X = Br, I). 1.1 equiv of $AgNO_3$ in methanol were added dropwise to a methanol solution of $Ru_2(\mu\text{-}O_2CCH_3)_4Cl$ in the dark. The precipitated AgCl was filtered over paper. 1.2 equiv of NaX (X = Br or I) in methanol were added dropwise in the dark with agitation. After 1 h of stirring, the precipitated AgX was filtered off, and the solvent was evaporated. The brown salt obtained was washed several times with water and dried in vacuo with NaOH.

Results

(1) Molecular and Electronic Structures of the Key Building Blocks. $[Ru_2(\mu\text{-}O_2CCH_3)_4]^+$, $[Ru_2(\mu\text{-}O_2CCH_3)_4(H_2O)_2]^+$, $Ru_2(\mu\text{-}O_2CCH_3)_4$, and $Ru_2(\mu\text{-}O_2CCH_3)_4(H_2O)_2$ have been considered as the key building blocks for axially linked extended materials. $[Ru_2(\mu\text{-}O_2CCH_3)_4]^+$ and $Ru_2(\mu\text{-}O_2CCH_3)_4$, even if not actually present as isolated units in any real compound, are realistic models for the $[Ru_2(\mu\text{-}O_2CR)_4]^{+/0}$ unit in extended systems. Both bis-aquo species have been structurally characterized;[52,53] different compounds containing the binuclear cation have been used as starting products for extended systems,[5a,6,30,54] owing to the lability of the axially coordinated water molecules.

As far as the cationic mixed-valent species are concerned, the main structural parameters for both species, as obtained from the geometry optimization, are given in the Supporting Information, Table S1. The Ru−Ru distance is 2.30 Å for the unsolvated species, and 2.34 Å for the bis-adduct. Both distances are in the range usually found for these systems, the calculated value being slightly longer than the experimental one (2.29 Å for the bis-adduct). This peculiarity has also been reported for other transition metal complexes. Cotton et al.[25a] showed that it seems to be a consequence of using an ECP (effective core potential) in the basis sets. All electron calculations produce better results but would be too computationally expensive for these systems. Vibrational normal modes (Supporting Information, Table S2) are also in agreement with the experimental ones. The calculated Ru−Ru stretching frequency is 330 cm^{-1} for $[Ru_2(\mu\text{-}O_2CCH_3)_4]^+$ and 340 cm^{-1} for $[Ru_2(\mu\text{-}O_2CCH_3)_4(H_2O)_2]^+$ while the experimental one is around 326 cm^{-1} for $[Ru_2(\mu\text{-}O_2CCH_3)_4(H_2O)_2]^+$[55] and 347–350 cm^{-1} for $[Ru_2(\mu\text{-}O_2CR)_4(Lax)]_\infty$ compounds[21] (Lax: bridging anionic axial ligand linked to Ru via oxygen atoms). The electronic structure for both species (Supporting Information, Figure S1) is in agreement with previous results and exhibits the already described near-degeneracy of the $\pi^*-\delta^*$ manifold.

The main structural parameters for the (II,II) complexes contained in Supporting Information, Table S3 are comparable to those calculated by Sizova[27] as are the vibrational normal modes in Supporting Information, Table S4. The Ru−Ru distance is 2.30 Å for the unsolvated species and 2.32 Å for the bis-adduct, slightly longer than the experimental 2.26 Å value (the same comment made for the mixed-valent species applies here). The calculated Ru−Ru stretching frequencies are 369 cm^{-1} and 374 cm^{-1}, respectively. These results are also in good agreement with the experimental results for pseudopolymeric $[Ru_2(\mu\text{-}O_2CR)_4]_\infty$ compounds:[21] about 350 cm^{-1}. The electronic structure for both species

(48) (a) Miertus, S.; Scrocco, E.; Tomasi, J. *Chem. Phys.* **1981**, *55*, 117. (b) Miertus, S.; Tomasi, J. *Chem. Phys.* **1982**, *65*, 239. (c) Cossi, M.; Barone, V.; Cammi, R.; Tomasi, J. *Chem. Phys. Lett.* **1996**, *255*, 327. (d) Mennucci, B.; Tomasi, J. *J. Chem. Phys.* **1997**, *106*, 5151. (e) Mennucci, B.; Cancès, E.; Tomasi, J. *J. Phys. Chem. B* **1997**, *101*, 10506. (f) Cammi, R.; Mennucci, B.; Tomasi, J. *J. Phys. Chem. A* **1999**, *103*, 9100. (g) Cossi, M.; Barone, V.; Robb, M. A. *J. Chem. Phys.* **1999**, *111*, 5295. (h) Cammi, R.; Mennucci, B.; Tomasi, J. *J. Phys. Chem. A* **2000**, *104*, 5631. (i) Cossi, M.; Barone, V. *J. Chem. Phys.* **2000**, *112*, 2427. (j) Cossi, M.; Barone, V. *J. Chem. Phys.* **2001**, *115*, 4708. (k) Cossi, M.; Rega, N.; Scalmani, G.; Barone, V. *J. Chem. Phys.* **2001**, *114*, 5691. (l) Cossi, M.; Scalmani, G.; Rega, N.; Barone, V *J. Chem. Phys.* **2002**, *117*, 43. (m) Cossi, M.; Rega, N.; Scalmani, G.; Barone, V. *J. Comput. Chem.* **2003**, *24*, 669.
(49) Flükiger, P.; Lüthi, H. P.; Portmann, S.; Weber, J. *MOLEKEL 4.0*; Swiss National Supercomputing Centre CSCS: Manno, Switzerland, 2000.
(50) Mitchell, R. W.; Spencer, A.; Wilkinson, G. J. *J. Chem. Soc., Dalton Trans.* **1973**, 846.
(51) Gritzner, G.; Kuta, J. *Pure Appl. Chem.* **1984**, 461.
(52) (a) Binont, A.; Cotton, F. A.; Felthouse, T. R. *Inorg. Chem.* **1979**, *18*, 2599; corrected by Marsh, R. E.; Schomaker, V. *Inorg. Chem.* **1981**, *20*, 303. (b) Drysdale, K. D.; Beck, E. J.; Cameron, T. S.; Robertson, K. N.; Aquino, M. A. S. *Inorg. Chim. Acta* **1997**, *256*, 243.
(53) Lindsay, A. J.; Wilkinson, G.; Motevalli, M.; Hursthouse, M. B. *J. Chem. Soc., Dalton Trans.* **1985**, 2321.
(54) Beck, E. J.; Drysdale, K. D.; Thompson, L. K.; Li, L.; Murphy, C. A.; Aquino, M. A. S. *Inorg. Chim. Acta* **1998**, *279*, 121.
(55) Clark, R. J. H.; Ferris, L. T. H. *Inorg. Chem.* **1981**, *20*, 2579.

Table 1. Comparison between Calculated (Vacuum) and Experimental Bond Distances (Å) and Angles for $[Ru_2(\mu\text{-}O_2CCH_3)_4X_2]^-$(X = Cl, Br, I)

	$[Ru_2(\mu\text{-}O_2CCH_3)_4Cl_2]^-$		$[Ru_2(\mu\text{-}O_2CCH_3)_4Br_2]^-$		$[Ru_2(\mu\text{-}O_2CCH_3)_4I_2]^-$	
	calculated	expt.	calculated	expt.	calculated	expt.
Ru−Ru	2.429	2.3069(8)[a] 2.3088(6)[b] 2.286(2)[c]	2.436	2.2999(16)[d] 2.2956(5)[e]	2.446	2.312(3)[f]
Ru−X	2.546 2.547	2.5396(15)[a] 2.5627(10)[b] 2.521(4)[c]	2.718 2.711	2.6763(14)[d] 2.6779(4)[e]	2.905 2.899	2.895(2)[f]
Ru−O[g]	2.07	2.029(4)[a] 2.026(3)[b] 2.01(1)[c]	2.07	2.027(5)[d] 2.027(2)[e]	2.07	2.035(14)[f]
Ru−Ru−X	174.57° 174.58°	177.29°(4)[a] 178.86°(3)[b] 176.2°(1)[c]	174.82° 174.69°	177.10°(6)[d] 177.12°(19)[e]	174.15° 173.88°	176.25°(11)[f]
O−Ru−Ru[g]	92°	89.80°(12)[a] 89.03°(8)[b]	92°	89.17°(15)[d] 89.19°(6)[e]	92°	89.16°(4)[f]

[a] Values for $NEt_4[Ru_2(\mu\text{-}O_2CCH_3)_4Cl_2]$.[39] [b] Values for $PPh_4[Ru_2(\mu\text{-}O_2CCH_3)_4Cl_2]$.[39] [c] Values for $Cs[Ru_2(\mu\text{-}O_2CCH_3)_4Cl_2]$.[52a] [d] Values for $NEt_4[Ru_2(\mu\text{-}O_2CCH_3)_4Br_2]$.[39] [e] Values for $K[Ru_2(\mu\text{-}O_2CCH_3)_4Br_2]$.[39] [f] Values for $PPh_4[Ru_2(\mu\text{-}O_2CCH_3)_4I_2]$.[39] [g] Mean values are reported as the deviation is under 2%.

(Supporting Information, Figure S2) exhibits the already described $(\pi^*)^2(\delta^*)^2$configuration.

(2) Trends along the $[Ru_2(\mu\text{-}O_2CCH_3)_4X_2]^-$ (X = Cl^-, Br^-, I^-) Series. $[Ru_2(\mu\text{-}O_2CCH_3)_4X_2]^-$. Molecular structures. Numerous halotetracarboxylatodiruthenium (II,III) complexes $Ru_2(\mu\text{-}O_2CR)_4X$ (X = halide, R = alkyl, aryl) have been synthesized and characterized. In the solid state, most of them show a polymeric structure where the binuclear units are linked by the halide ligands giving zigzag or linear chains.[3,6] When dissolved, neutral discrete $[Ru_2(\mu\text{-}O_2CMe)_4XSv]$ units, with one axial position occupied by one halogen atom and the other one by a solvent molecule (Sv), have been reported in most common solvents except for water or methanol, where cationic $[Ru_2(\mu\text{-}O_2CMe)_4(Sv)_2]^+$ species[3,17,56] have been identified. Despite the fact that anionic tetracarboxylatodiruthenium(II,III) complexes have been more scarcely reported, they were selected for this first study because simulating the polymeric arrangement represents a substantially harsher challenge. Recently, Barral et al. published X-ray studies of these anionic units where both axial positions are occupied by the halide ligands;[39] therefore, we will use these results to compare with the calculated data. Shown in Table 1 are the structural parameters of the optimized geometry for $[Ru_2(\mu\text{-}O_2CCH_3)_4Cl_2]^-$, $[Ru_2(\mu\text{-}O_2CCH_3)_4Br_2]^-$, and $[Ru_2(\mu\text{-}O_2CCH_3)_4I_2]^-$ compounds, respectively, along with the available experimental data.

It can be observed in Table 1 that the optimized parameters are in excellent agreement with the experimental values except for the slightly longer Ru−Ru distance obtained. We will show later on that our theoretical calculations are capable of reproducing many other experimental properties. The Ru−Ru fundamental stretching has been experimentally detected at about 325–340 cm^{-1} for both $[Ru_2(\mu\text{-}O_2CR)_4Cl]_\infty$, $[Ru_2(\mu\text{-}O_2CR)_4Cl_2]^-$, $[Ru_2(\mu\text{-}O_2CR)_4Br]_\infty$, and $[Ru_2(\mu\text{-}O_2CR)_4Br_2]^-$ compounds;[56,57] we calculated it at 344, 339, and 347 cm^{-1} for $[Ru_2(\mu\text{-}O_2CR)_4Cl_2]^-$, $[Ru_2(\mu\text{-}O_2CR)_4Br_2]^-$, and $[Ru_2(\mu\text{-}O_2CR)_4I_2]^-$, respectively.

$[Ru_2(\mu\text{-}O_2CCH_3)_4X_2]^-$. Electronic Spectra. We measured the solution UV–vis spectra for the $[Ru_2(\mu\text{-}O_2CCH_3)_4X_2]^-$ species, generated by simply dissolving the corresponding $Ru_2(\mu\text{-}O_2CCH_3)_4X$ compound in acetonitrile (approximately 2×10^{-4} M) containing an excess TBAX, to ensure that both axial positions are occupied by X^-. The solvent of choice was acetonitrile as all the complexes are adequately soluble, and it does not replace the halide in the axial position.[56] The measured spectra are shown in Figure 1.

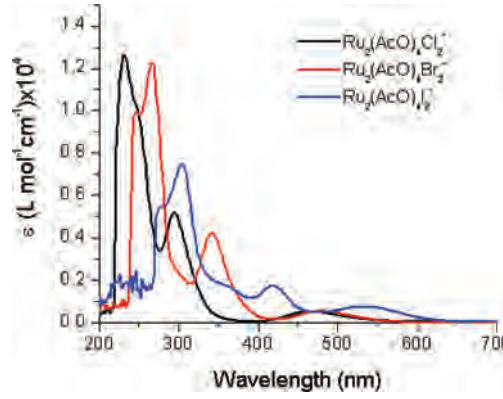

Figure 1. Experimental UV–vis spectra for $[Ru_2(\mu\text{-}O_2CCH_3)_4X_2]^-$ in acetonitrile with an excess of TBAX (X = Cl, Br, I).

A strong red shift of the bands situated in the UV region can be easily observed, whereas the visible absorption bands are only weakly sensitive to the axial ligand. The latter appeared at 464–468 nm for the chloro derivative, it is slightly red-shifted for the bromine derivative (474–480 nm), and it shows a greater shift for the iodine derivative 545–566 nm. The data obtained is fully consistent with previous publications[39,56] where a clear trend, when changing the halogen ligand, was reported.

The higher energy UV band is usually assigned to a LMCT $\sigma(X) \rightarrow \sigma^*(Ru_2)$ transition[56] while the other one is assigned to a $\pi(X) \rightarrow \pi^*(Ru_2)$ transition. The band appearing at 460–550 nm is usually assigned to $\pi(RuO,Ru_2) \rightarrow \pi^*(Ru_2)$ transition. These are the only bands with significant intensity in the spectra which were recorded up to 800 nm. However, other bands at 630–700 nm and around 1130 nm were previously reported and assigned to the $\sigma(X) \rightarrow \pi^*(Ru_2)$ and $\delta(Ru_2) \rightarrow \delta^*(Ru_2)$ transitions, respectively. We will discuss these assignments in the next section.

(56) Miskowski, V. M.; Gray, H. B. *Inorg. Chem.* **1988**, *27*, 2501.

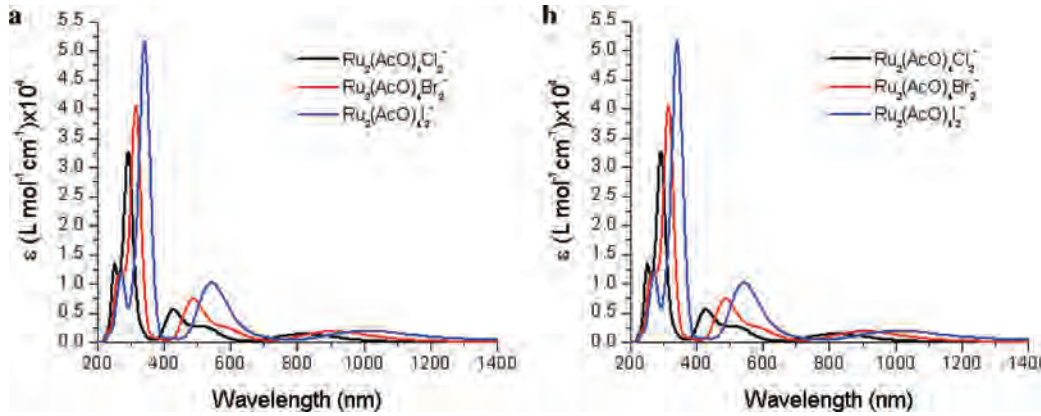

Figure 2. Calculated UV–vis spectra for $[Ru_2(\mu\text{-}O_2CCH_3)_4X_2]^-$ (X = Cl, Br, I) (a) for the unsolvated species (TDDFT) and (b) for the solvated species in acetonitrile (TDDFT-PCM).

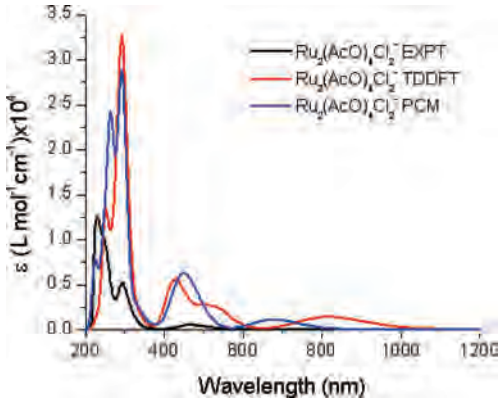

Figure 3. Experimental and calculated (both solvated and unsolvated) UV–vis spectra for $[Ru_2(\mu\text{-}O_2CCH_3)_4Cl_2]^-$.

We simulated the electronic spectra from the optimized molecular geometries. The spectra obtained for the three compounds are shown in Figure 2a where the expected red shift is observed. The only difference between the experimental and the simulated results is that the theory predicts a significant shift of the visible band when going from Cl to Br that is not observed in the experiment.

We also performed a series of TDDFT-PCM calculations to evaluate the influence of the solvent on the computed spectra. These are shown in Figure 2b. Despite a very slight blue shift in the NIR bands, the spectra calculated in vacuum and in solution do not differ significantly from each other, and we can still clearly observe the red shift shown in the experiment along the Cl−Br−I series.

The experimental spectrum for each compound is satisfactorily reproduced by the calculations though we do observe increasing differences while moving from Cl to I. The experimental spectrum and both calculated spectra for $[Ru_2(\mu\text{-}O_2CCH_3)_4Cl_2]^-$ are superimposed in Figure 3.

$[Ru_2(\mu\text{-}O_2CCH_3)_4X_2]^-$. Electronic Structure. To understand more deeply the nature of the observed transitions, we will discuss in detail the electronic structure of $[Ru_2(\mu\text{-}O_2CCH_3)_4Cl_2]^-$ in vacuum and in solution.

For this complex, both electronic structure calculations are presented in an open-shell MO diagram (Figure 4) while selected MOs are shown in Figure 5.

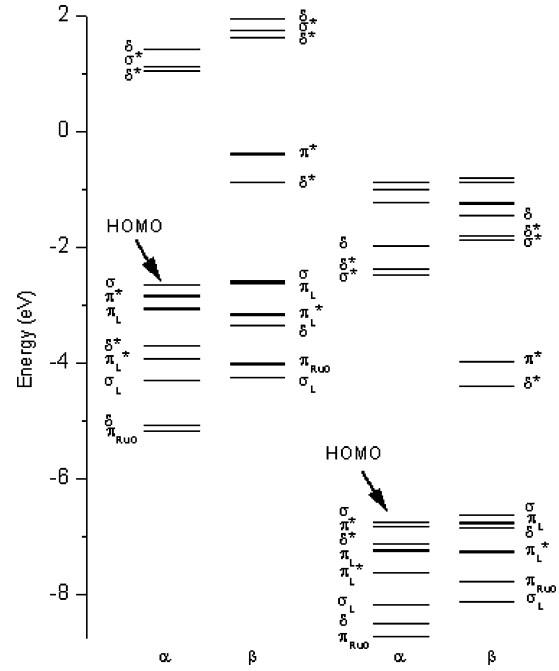

Figure 4. Open-shell electronic structure calculations for $[Ru_2(\mu\text{-}O_2CCH_3)_4Cl_2]^-$ in vacuum (left) and in solution (right).

In vacuum, the highest occupied molecular orbital (HOMO) σ of both the α and β manifold, found at −2.6 eV, is a combination of the d_{z^2} on the Ru and the p_z orbitals on the Cl. This orbital can be described as being doubly occupied because its α and β components have the same spatial part and are almost degenerate.

This structure is consistent with previous publications[19,21,27] that assign the magnetic orbitals as being of δ^* and π^* Ru_2 character.

When including the solvent, all the orbitals shift to lower energies. The order of the orbitals is slightly altered. In the α manifold, the δ^* now appears at higher energy than the π_L on the Cl. On the other hand, the δ orbitals in the β manifold appear at higher energy than the π_L^*. This can be more clearly observed in Figure 4.

The electronic structure calculations of the three complexes in vacuum are presented in an open-shell MO diagram (Figure 6) to illustrate the differences when changing the axial ligand. The order of the MOs is essentially the same

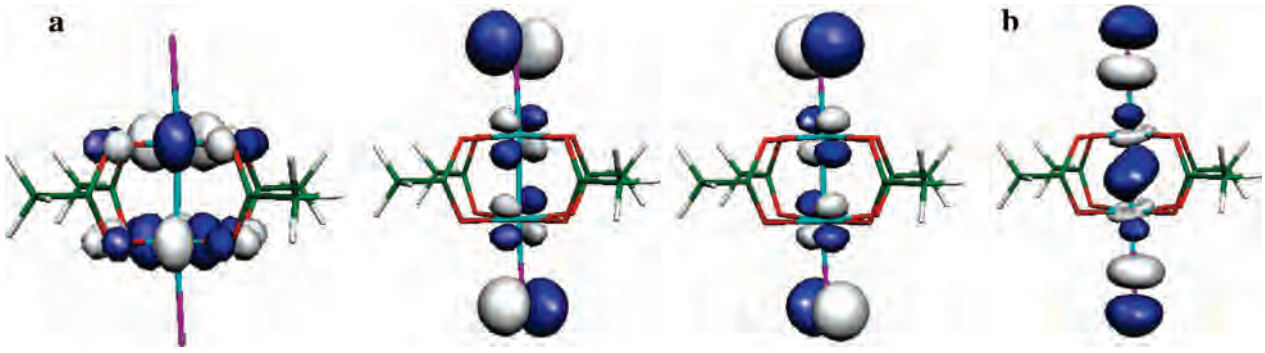

Figure 5. Selected α MOs for $[Ru_2(\mu\text{-}O_2CCH_3)_4Cl_2]^-$ in vacuum (a) singly occupied molecular orbitals (SOMOs) δ^* and both π^* (b) HOMO σ.

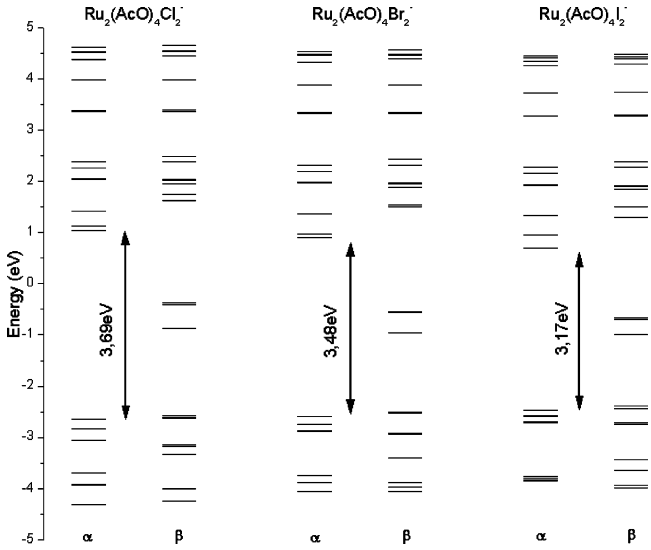

Figure 6. Electronic structure calculations of $[Ru_2(\mu\text{-}O_2CCH_3)_4X_2]^-$ (X = Cl, Br, I) performed in vaccum.

Table 2. Relevant Calculated Optical Transitions for $[Ru_2(\mu\text{-}O_2CCH_3)_4Cl_2]^-$

TDDFT				TDDFT-PCM			
λ (nm)	f	assign.	%	λ (nm)	f	assign.	%
812.4	0.018	$\pi_L \rightarrow \pi^*$	46	680.0	0.015	$\pi_L \rightarrow \pi^*$	52
		$\sigma \rightarrow \sigma^*$	34			$\sigma \rightarrow \sigma^*$	33
		$\delta \rightarrow \delta^*$	22			$\delta \rightarrow \delta^*$	11
529.5	0.026	$\sigma \rightarrow \sigma^*$	84	475.0	0.042	$\sigma \rightarrow \sigma^*$	99
		$\pi_{RuO} \rightarrow \pi^*$	11				
473.5	0.020	$\pi_{RuO} \rightarrow \pi^*$	58	439.2	0.062	$\pi_{RuO} \rightarrow \pi^*$	70
		$\sigma \rightarrow \sigma^*$	22			$\sigma \rightarrow \sigma^*$	17
425.7	0.071	$\sigma_L \rightarrow \pi^*$	80	332.6	0.015	pO $\rightarrow \pi^*$	92
300.8	0.113	$\pi^* \rightarrow$ pCO	62	331.9	0.015	pO $\rightarrow \pi^*$	92
297.8	0.017	$\pi^* \rightarrow$ pCO	92	293.9	0.353	$\sigma \rightarrow \sigma^*$	47
						$\pi_{RuO} \rightarrow \pi^*$	46
292.7	0.251	$\pi^* \rightarrow$ pCO	35	266.2	0.13	$\delta \rightarrow$ pCO	95
286.9	0.024	$\pi_L \rightarrow$ pCO	57	265.2	0.15	$\pi_{RuCO} \rightarrow \pi^*$	50

for the three species but the energy gaps are smaller while moving from Cl to I. For instance, for the α manifold, the $\sigma-\sigma^*$ gap differs by 0.52 eV between one compound and the other. These differences are significant to understand the different electronic spectra obtained.

The most representative calculated optical transitions for $[Ru_2(\mu\text{-}O_2CCH_3)_4Cl_2]^-$ (see Figure 3) are collected in Table 2, while a complete list of relevant calculated optical transitions for all complexes is available in the Supporting Information, Table S5. We will discuss the TDDFT-PCM calculation as it most nearly represents the real system.

The calculated transition appearing at 681.0 nm, the only one with significant intensity above 600 nm, has a mixed character: $\pi_L \rightarrow \pi^*$ (52%), $\sigma \rightarrow \sigma^*$ (33%), and $\delta \rightarrow \delta^*$ (11%). This band was not observed when measuring the electronic spectra as it is reported to have a very small extinction coefficient.

The absorption at 460 nm is not originated by a single transition but is composed by two transitions of mixed character. The most intense transition composing this band has a dominant $\pi_{RuO} \rightarrow \pi^*$ character, consistent with previous assignments.

Below 350 nm, the calculations predict a very large number of allowed transitions of significant intensity. This is consistent with the experimental spectrum which shows two intense bands in this region. The assignment of these bands is rather difficult as they are composed by a number of overlapping transitions including the expected LMCT $\sigma \rightarrow \sigma^*$ transition. One previous assignment[56] of one these bands to a LMCT $\pi_L \rightarrow \pi^*$ transition, on the basis of its low intensity compared to that of the $\sigma \rightarrow \sigma^*$ transition found in related Rh compounds, is not supported by our calculations as this transition appears at much lower energies, in agreement with the prediction by Norman and co-workers.[19] The assignment for the other two complexes can be equivalently analyzed.

$[Ru_2(\mu\text{-}O_2CCH_3)_4X_2]^-$. Electrochemistry. CV studies on this series of compounds show a quasi-reversible one-electron reduction that becomes less reversible when going from Cl to I. The $Ru_2^{5+/4+}$ couple for $[Ru_2(\mu\text{-}O_2CCH_3)_4Cl_2]^-$ was experimentally measured at $E_{1/2} = -0.97$ vs Fc ($E_{1/2} = -0.46$ vs Ag/AgCl) which is consistent with previous results reported for the same complex.[57] For the other complexes, an anodic shift was observed (Br, −0.71 V; I, −0.74 V vs Fc) which generally suggests a weaker donor ligand.[57] Indeed, this shift in $E_{1/2}$ roughly agrees with the variation in the donor number (DN) of the axial ligand (DN in acetonitrile = 34.9, 32.5, and 27.7 for Cl^-, Br^-, and I^-, respectively[58]), an expected trend already found for N-coordinating axial ligands.[57] Such a dependence of $E_{1/2}$ on DN is consistent with both the energy shift of the δ^* MO (where the additional electron is supposed to be added) when moving from

(57) Vamvounis, G.; Caplan, J. F.; Cameron, T. S.; Robertson, K. N.; Aquino, M. A. S. *Inorg. Chim. Acta* **2000**, *304*, 87.
(58) Linert, W.; Jameson, R. F.; Taha, A. *J. Chem. Soc., Dalton Trans.* **1993**, 3181.

Table 3. Mulliken Atomic Charge and Mulliken Atomic Spin Densities on Ru for Calculations on Unsolvated Complexes

	total charge	spin density
$[Ru_2(\mu\text{-}O_2CCH_3)_4Cl_2]^-$	0.31	1.34
$[Ru_2(\mu\text{-}O_2CCH_3)_4Br_2]^-$	0.33	1.30
$[Ru_2(\mu\text{-}O_2CCH_3)_4I_2]^-$	0.34	1.28

the Cl^- derivative to the heavier Br^- or I^- ones, and with the variation of the resulting total electronic density at the Ru−Ru center (see Table 3). The latter is a result of both σ effects (the electronic density distribution at the σ, σ^* Ru−Ru MO) and π effects (π^* and δ^* MO lower in energy for the Br^- and I^- derivatives than for the Cl^- derivative because of both lower overlap and lower energy matching). Reduction potentials were not calculated as the uncertainty of the method for ruthenium complexes has been reported to be between 0.2 and 0.6 eV[59] which is larger than the potential variation along our series.

(3) Conformation of $[Ru_2(\mu\text{-}O_2CCH_3)_4Cl]_nCl^-$ Oligomers As Models for Coordination Polymers: Insights into the Crystalline Polymorphism and Liquid Crystalline Supramolecular Structure. As mentioned in the Introduction, the conformation of $[Ru_2(\mu\text{-}O_2CR)_4Cl]_\infty$ extended strands may vary significantly from one homologue to the other, from the crystalline to the liquid-crystalline phase, and even from one crystalline polymorph to the other for the same compound. Different crystallized analogues[3,6] show Ru−Cl−Ru angles in the range of 115–180°; estimates in the LC phase[29,40] gave values ranging from 110° to 120°. As these structural features have been shown to determine some of the physical properties of these materials (e.g., the extent of the magnetic interaction between adjacent units), it is important to understand the factors (packing, orbital overlap, microsegregation) that determine the conformation.

With this objective, we optimized the geometry of two oligomers: $[Ru_2(\mu\text{-}O_2CCH_3)_4Cl]_2Cl^-$ (dimer) and $[Ru_2(\mu\text{-}O_2CCH_3)_4Cl]_3Cl^-$ (trimer). Their geometries converged to zigzag structures with angles 146° for the dimer and 144°−145° for the trimer (Figure 7, Supporting Information, Table S6). In other words, QM calculations predict zigzag conformations for both oligomers, with Ru−Cl−Ru angles about 145°. As we are not considering a lattice, packing is not the main issue to be considered when trying to understand why the zigzag conformation prevails over the linear one; indeed, orbital overlap seems to have an important contribution on this matter.

The only compound for which such angle value has been crystallographically found is $Ru_2(\mu\text{-}O_2C(CH_2)_3CH_3)_4Cl$ (142°),[3,6,31] the higher homologue whose structure has been solved. An examination of the published crystallographic structures of $[Ru_2(\mu\text{-}O_2CR)_4Cl]_\infty$ compounds reveals that most of the solved structures show Ru−Cl−Ru angles within the 118–125° range, which we will call the "bent" conformation. All these cases correspond to compounds where the equatorial carboxylates possess short aliphatic chains (≤4 C atoms) or long (6 C atoms) but rigid aliphatic chains.[60] Short chain derivatives[52a,61,62] also presented the "linear" strand conformation (Ru−Cl−Ru angle of 180°), which was also achieved with bulky and rigid derivatives.[63]

$Ru_2(\mu\text{-}O_2C(CH_2)_3CH_3)_4Cl$ seems unique in the sense it is the only compound with "flexible" long aliphatic chains for which the structure has been solved, and it is the only one for which the Ru−Cl−Ru angle approaches the value obtained from QM geometry optimizations. There might be a connection between these two facts.

To estimate the amount of energy that would be required to straighten the oligomer, the potential energy surface (PES) when moving the Ru−Cl−Ru angle between 130° to 180° was explored (Figure 8). We found that only 1.5 kcal/mol was required to move along the surface from the zigzag "ideal angle" conformation (ca. 145°) to either the "linear"

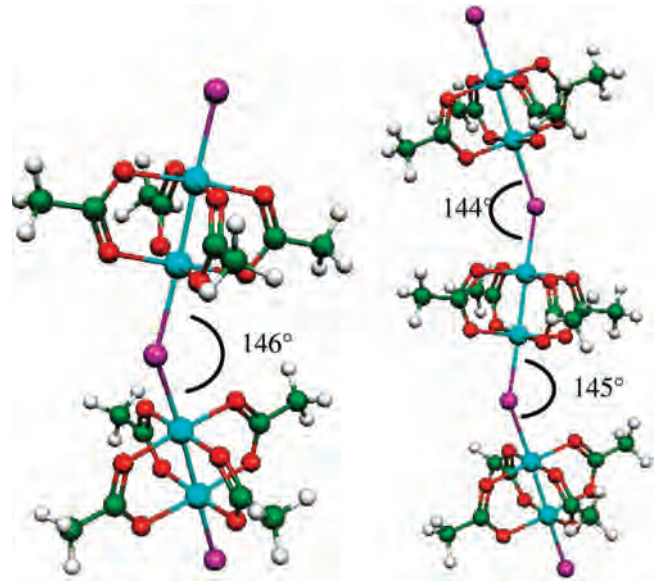

Figure 7. Optimized oligomers: $[Ru_2(\mu\text{-}O_2CCH_3)_4Cl]_2Cl^-$ (dimer, left) and $[Ru_2(\mu\text{-}O_2CCH_3)_4Cl]_3Cl^-$ (trimer, right) which presented a zigzag structure. Color code: Ru, turquoise; Cl, purple; O, red; C, green; H, white.

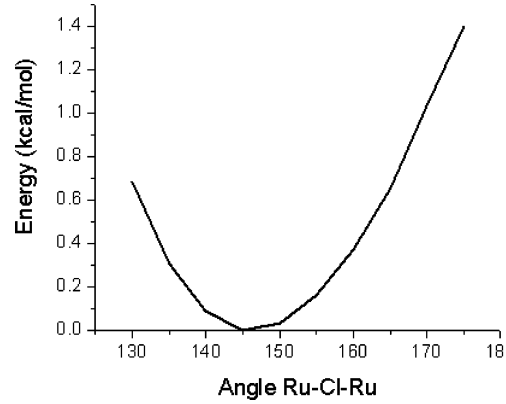

Figure 8. Relaxed scan of the PES when moving the Ru−Cl−Ru angle between 130° to 180° for $[Ru_2(\mu\text{-}O_2CCH_3)_4Cl]_2Cl^-$.

(59) Chiorescu, I.; Deubel, D. V.; Arion, V. B.; Keppler, B. K. *J. Chem. Theory Comput.* **2008**, *4*, 499–506.
(60) Barral, M. C.; Jiménez-Aparicio, R.; Pérez-Quintanilla, D.; Priego, J. L.; Royer, E. C.; Torres, M. R.; Urbanos, F. A. *Inorg. Chem.* **2000**, *39*, 65–70.
(61) Miskowski, V. M.; Loher, T. M.; Gray, H. B. *Inorg. Chem.* **1987**, *26*, 1098.
(62) Martin, D. S.; Newman, R. A.; Vlasnik, L. M. *Inorg. Chem.* **1980**, *19*, 3404.
(63) Cotton, F. A.; Kim, Y.; Ren, T. *Polyhedron* **1993**, *12*, 607.

one (180°) or the zigzag "bent" conformation (ca. 120°). This energy can be overcome by some packing constraints and is close to the energy corresponding to trans-gauche transitions at the aliphatic chains (ca. 0.8–0.9 kcal/mol of CH_2 units). Interestingly, the structure of $Ru_2(\mu\text{-}O_2C(CH_2)_3CH_3)_4Cl$ exhibits gauche conformations at C2−C3 bonds of two of the four aliphatic chains. These results allow an interpretation for the suggested connection between the length of the equatorial aliphatic chain and the Ru−Cl−Ru angle. We suggest that the packing requirements can be considered of slightly higher energy than the energetic barrier for the conformational changes in the coordination strands and that they can only be balanced by conformational arrangements of the aliphatic chains provided the aliphatic chains are long enough. We are currently investigating this point in some more detail by means of both molecular mechanics calculations and crystallographic studies on longer homologues.

Conclusions

We performed DFT open shell calculations, including full geometry optimization, electronic structure, and normal modes determinations, for paramagnetic diruthenium tetracarboxylates of differing complexity: unsolvated species, axially coordinated bis-adducts, and oligomers. Our calculations reproduced well the known structural features of these compounds, as well as their electronic spectra and vibrational frequencies. Our calculations on the bis-adducts helped the interpretation of some experimental trends along the halogen series. The calculations on oligomers provided insights on the factors determining the polymeric strand conformation which, stated before, is a key parameter in determining some of their physical properties. We will next apply the same calculation methodology to predict selected physicochemical properties of not-yet synthesized compounds of this same family. This is part of a systematic search for the best combinations of molecular parts aimed to exhibit long axis electron delocalization.

Acknowledgment. This paper is dedicated to the memory of Prof. F. A. Cotton. We thank Leonardo Slep for critical reading of the manuscript and Pascale Maldivi for useful discussions with M.A.C. Financial support from UBACyT (X219) and ANPCyT (PICT 25409) is acknowledged. M.A.C. thanks Conicet for a doctoral fellowship. F.D.C. is a member of the scientific staff of Conicet. A.E.R. thanks the Fulbright commission for a Senior Fellowship to spend the summer of 2006 in Argentina. Computer resources were provided by the Large Allocations Resource Committee through Grant TG-MCA05S010 to A.E.R. The authors acknowledge the University of Florida High-Performance Computing Center (URL: http://hpc.ufl.edu) for providing computational resources and support that have contributed to the research results reported within this paper.

Supporting Information Available: Tables and figures with bond distances, bond angles, calculated IR-Raman vibrational modes, electronic structures, and calculated optical transitions (PDF). This material is available free of charge via the Internet at http://pubs.acs.org.

IC702505Z